Elastomers for Control of Wafer Temperature in the $\approx 50^{\circ}$C Range During High Dose Ion Implantation

Jeff Springer and Walt Wriggins
CORE Systems, Fremont, CA USA
jspringer@coresystems.com

Juergen Kusterer and Karl Zotter
Texas Instruments, Freising, Germany
j-kusterer@ti.com, k-zotter@ti.com

Michael I. Current
Current Scientific, San Jose, CA USA
currentsci@aol.com

***Abstract*- Wafer/pad temperatures are measured for various elastomer materials for control of wafer temperatures during high-power implantation to less than 40 C. Wafer/pad temperatures during and directly following implant are monitored by in-situ IR sensors and tracked over long operational cycles. Beneficial effects of wafer temperature control is noted for gain characteristics of modern IC devices.**

Keywords—elastomers, heat transfer, high power implantation, IR wafer temperature sensing.

I. INTRODUCTION

The effects of wafer temperature during implantation on damage accumulation in Si is well known at elevated (300 to 800 C) and "cryo" (0 to -100 C) temperatures [1,2]. It is far less widely known that, for certain IC device types, control of implant temperature in the regime near room temperature can also have a similarly significant effect on damage accumulation, dopant activation and device performance.

Silicone elastomers composed of Polydimethyl Siloxane (PDMS) with various crosslinked densities and filler additives have been used as heatsink pads in batch ion implanters for several decades. Desirable elastomer properties include: low outgassing in vacuum, stability at operating temperatures, no transfer of elemental contaminants to wafer backsides, low thermal resistance, excellent mechanical wear resistance and stability over thousands of wafer moves. Of critical importance here is the intimate contact of the wafer backside to the implanter wheel wafer mounts for high thermal conductivity. Customizing elastomers for reduced wafer temperatures during high-power implants requires management of all of these elastomer properties.

A local, 1-D description of the heat flow per unit time, dQ/dt, from the beam energy deposited in the photoresist (PR) and wafer layers is $\Sigma \{-\kappa * A * (\Delta T/\Delta X)\}$, where Σ is a sum through the stack of layers and interfaces from the wafer to the coolant flow region in the wafer mount, κ (W/m-K) is the heat conductivity of each layer and interface, A (m^2) is the conducting area, ΔT (K) is the temperature difference across an interface or a layer of thickness ΔX (m).

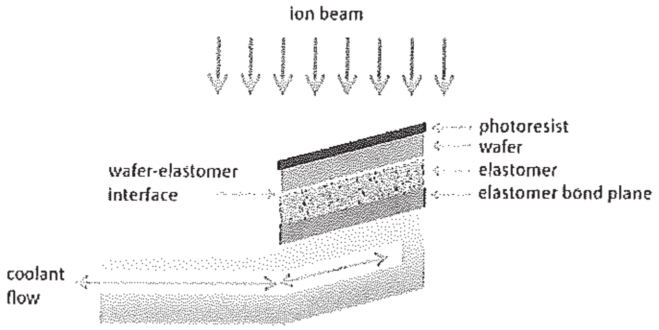

Fig. 1. Sketch of wafer pad assembly on spinning disk wafer pedestal showing major components of the heat transfer stack.

An additional complication, not treated here, is the dynamic heat load on various locations on the PR/wafer surface as the wafer is scanned in front of a finite sized ion beam at various speeds in various directions [3].

The two key factors in the 1-D heat flow model are (1) the heat conductivity of the various layers and interfaces and (2) the effective area of contact, A, at the various interfaces. Although Si wafers are much thicker (725 to 775 um) than typical elastomer layers, the high (149 W/m-K) thermal conductivity of Si shifts attention to the conductivity and wafer contact efficiency of the elastomer design.

II. IN-SITU TEMPERATURE SENSING

Local wafer temperatures were monitored during and directly after completion of high-power, high-dose implants by a variety of IR sensors and "wax dot" temperature markers. IR sensors included a forward-looking IR (FLIR) camera as well as a proprietary local IR in-situ sensor system [4]. The FLIR camera images show that the wafer pad temperatures at the elastomer/wafer interface were non-uniform during the early stages of cool down, indicating higher heat conductivity along the center of the wafer pad above the coolant flow lines (Figs. 2 & 3).

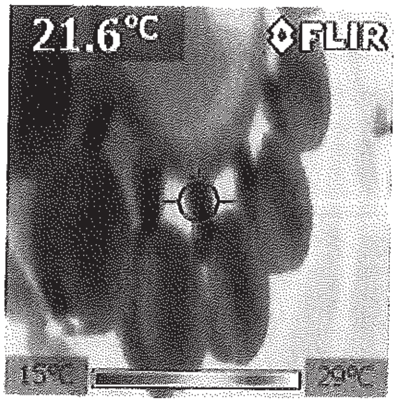

Fig. 2. FLIR sensor image of wafer wheel temperatures with a chiller flow at 13 C during early stages of cool down. Note cooler wafer pad regions along center radial regions with higher heat conductivity under the pad.

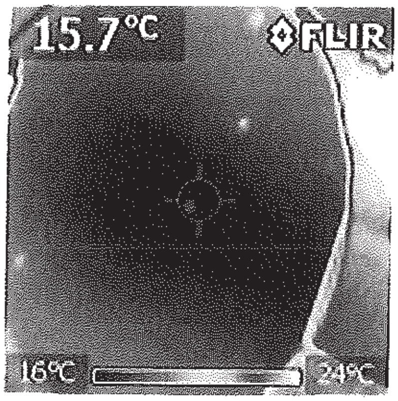

Fig. 3. FLIR sensor image of a single wafer pad temperatures with a chiller flow at 13 C during early stages of cool down. Note cooler wafer pad regions along center radial regions with higher heat conductivity under the pad.

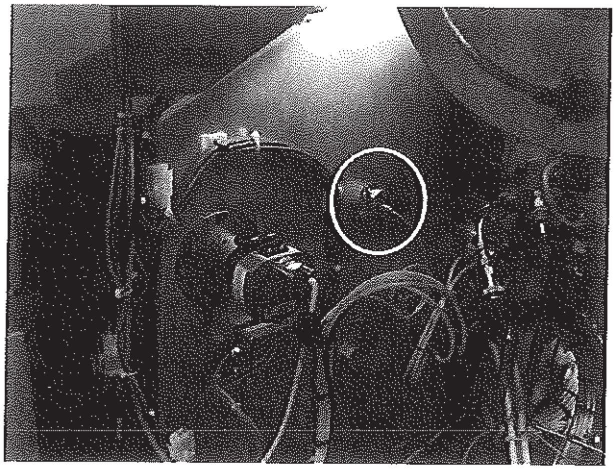

Fig. 4. Process chamber back of a GSD end station with an in-situ IR temperature sensor (circled) installed.

The in-situ IR sensor was mounted in the back of the process chamber of the ion implanter and continuously sampled wafer temperatures during the implant. The sensor head had a response time of 3 ms and a spectral range of 8-14 μm, which provided measurements of individual wafer/pad temperatures at a wheel rotation rate of 1200 rpm. During implantation, the IR sensor system recorded the peak temperature value which was then processed to deliver min, max and exponential moving average temperature values for further analysis. The area scanned by the IR sensor during implantation and wheel rotation and scanning is shown in Fig. 5.

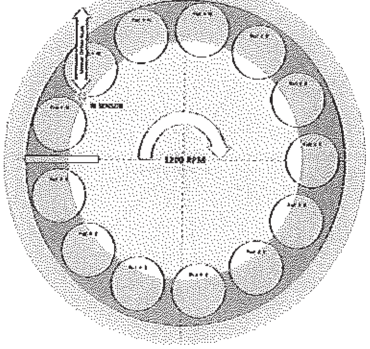

Fig. 5. Process disk showing 13 wafer pedestals. Shaded area indicates the observed area of the IR sensor during the scan and rotation of the disk.

During implant the maximum temperature was sampled to identify any temperature outliers using a repeated peak hold function. A single warm wafer would drive up the maximum temperature measurement and indicate a cooling problem.

III. ELASTOMER PERFORMANCE

The relevant elastomer characteristics for heat transfer from wafers are thermal conductivity, thickness, surface topology, hardness, and elongation. The balance needed to optimize these factors is far from obvious [5].

To increase the thermal conductivity of a siloxane elastomer above the typical ≈0.2 W/m-K value, it must be filled with materials with higher thermal conductivity, i.e. carbon, alumina, etc. Unfortunately, to achieve above 0.4 W/m-K, one must put large amounts of filler (>35 wt %) into the elastomer matrix. Filler addition at this level hardens the elastomer material, producing a stiffer, less-conformal wafer-elastomer contact and poorer thermal transfer.

Elastomer thickness is difficult to manipulate to increase wafer cooling efficiency. Typical elastomer thicknesses range from 3 to 12 mils (76 to 305 um). The elastomer thickness in this work was approximately 4 mils (102 um).

The elastomer surface topology must be designed to provide sufficient contact to the wafer backside for efficient cooling. However, one must limit the wafer/pad contact area to avoid wafers sticking during removal after implantation. Typical elastomer surface topography has roughness Ra value of 100 micro inch (2.5 um).

The hardness test (ASTM D2240) for elastomer materials uses a sharp tipped steel probe that actually tears through the surface and penetrates the elastomer. The depth level of penetration into the material is then converted into a hardness value. This hardness test is called a "Shore" procedure, named for the original developer, and elastomers are a "type A" material in this context [6]. Correlation of the hardness test values with elongation testing data is essential. Elongation measurement of elastomers is based upon ASTM D412 procedures. In this test, the elastomer is stretched until failure occurs. Elongation over 100% is highly desired. When elongation and hardness are at appropriate values, this results in an elastomer that can conform to the wafer backside efficiently under the centrifugal forces driven by the implant disk spinning. In two-component siloxane formation, manipulation of the elastomer crosslink density is adjusted via off-ratio stoichiometry to achieve the proper balance of elongation and hardness characteristics.

Our first approach to modify a standard siloxane elastomer was to increase the thermal conductivity by the addition of high thermal conductance particles. The estimated thermal conductivity of the version-1 elastomer was ≈0.5 W/m-K. However, the added filler materials stiffened the elastomer material and lowered the elongation potential so the wafer-elastomer contact was severely degraded. In-situ infrared temperature measurements showed wafer temperatures >62 C with a beam power of 1.7 kW. This was 14 C hotter than the OEM standard disk elastomer.

The next approach started with relatively un-loaded silicone material, (k≈0.2 W/m-K), with improved wafer-elastomer contact properties. The version-2 elastomer layer had a Shore A hardness of ≈30 and elongation over 100%. Testing of the version-2 disk pads resulted in a 14 C wafer-pad temperature drop below the performance of a standard elastomer. The tool engineers nicknamed this elastomer as the "Eskimo" due to this outstanding temperature reduction. (Fig. 6).

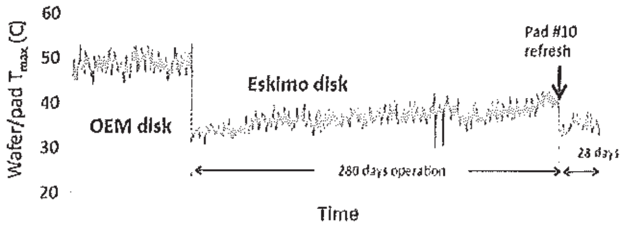

Fig. 6. Peak wafer/pad temperatures, T_{max}, over a ≈400 day period including a change from the OEM to the CORE "Eskimo" elastomer disk. The initial temperature drop for a 1.2 kW beam power implant was ≈15° C, with T_{max} remaining under 40 C for over 250 days. After 280 days of operation, T_{max} returned to ≈35 C after an in-situ refresh of a single pad (#10) exposed to beam heat and UV radiation during idle modes.

Over the course of 280 days of full operation, the Eskimo disk showed a slow, but steady, rise in peak wafer/pad temperature over time. Close examination showed that the major driver for this temperature rise was a single pad, #10, which was exposed to heat and UV radiation from the idle ion beam while the machine was between wafer runs with no wafers loaded on the disk. The resulting hardening of the polymer surface degraded the wafer/elastomer heat transfer characteristics. A simple surface treatment recovered most of the elastomer performance to its original state (see Fig. 6). The systematically superior cooling of the Eskimo elastomer disk was confirmed by average wafer/pad temperature measurements at beam powers of 600 to 1500 W (Fig. 7).

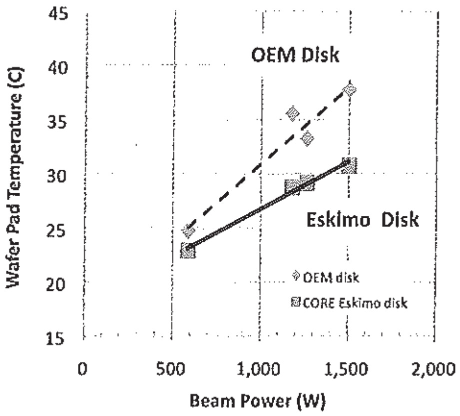

Fig. 7. Average wafer/pad temperatures for OEM and Core "Eskimo" elastomer disks for beam powers between 588 and 1,500 W. Doses ranged from 3e15 to 1.2e16 ions/cm^2 and energies from 60 to 150 keV for these tests.

IV. TEMPERATURE UNIFORMITY

The wafer/pad temperatures remained stable for several minutes before cooling down after the end of the implant. The individual pad characteristics could then be examined directly after high power implants (Fig. 8). These IR measurements, showing an OEM pad temperature difference of ≈11 C over a disk, were confirmed by additional use of temperature stickers and detailed examination of the electrical device data. However the Eskimo disk pads showed a consistently lower and much more uniform wafer/pad temperature of ≈18 C, indicating a remarkably improved heat transfer between wafer and pedestal.

V. DEVICE RESULTS

One of the critical device parameters linked to the wafer temperature during ion implantation is the resulting bipolar transistor gain h_{FE}. The enhanced cooling performance of the Eskimo disk pads leads to a 9% higher transistor gain compared to operation with an OEM disk (Fig. 9). Note that although the temperature scale in Fig. 9 is the measured average pad temperatures at a high power (1.5 kW) implant (see Fig. 7), the transistor bipolar gain, h_{FE}, is the result of multiple implant steps at various beam powers (also shown in Fig. 7). There are many other IC fabrication steps that influence h_{FE} values in addition to ion implantation. However, lots processed directly after the installation of the Eskimo elastomer disk showed the marked improvement in h_{FE} shown in Fig. 9.

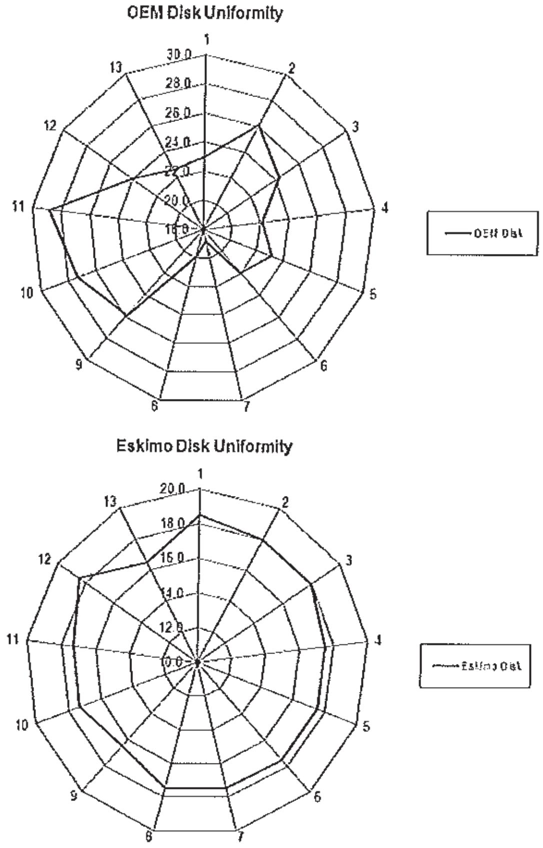

Fig. 8. Individual wafer/pad temperatures measured in-vacuum with the IR sensor immediately after completion of a high power implant for wafers on the OEM (upper) and Eskimo (lower) disks. Note the different temperature scales in the two spider web plots. The OEM disk showed wafer/pad temperatures between 19°C and 29°C over the 13 disk positions. The Eskimo disk showed a much tighter distribution of wafer/pad temperatures, between 17°C and 18.5°C over the disk positions.

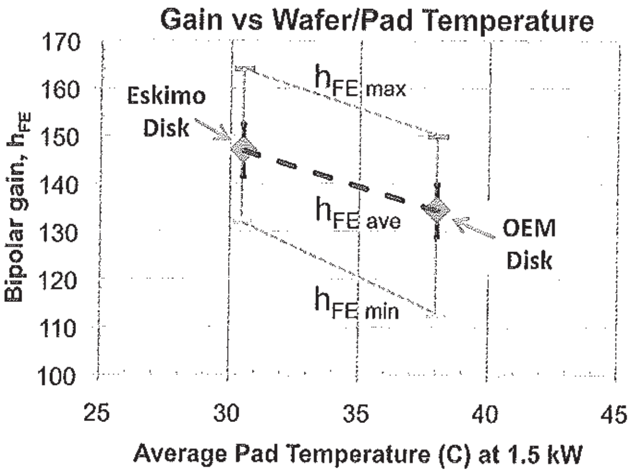

Fig. 9. Bipolar gain, h_{fe}, data for the Eskimo and OEM discs plotted at the average pad temperature for a 1.5 kW implant. Also shown are the maximum, minimum and standard deviation values for h_{fe}. The average transistor hybrid forward emitter gain of this device improved by more than 9% using the Eskimo disk compared to a standard OEM disk.

The carrier-defect interactions leading to the gain shift shown in Fig. 9 likely involve changes in the minority carrier recombination rates and mobility effects from carrier scattering. The results shown here and the related data in Ref. 4 clearly show a systematic increase in bipolar gain with cooler wafer temperatures for high-dose implants. Understanding these results in view of the general increase in damage accumulation rates for lower implant temperatures [7,8] will be a challenge.

VI. SUMMARY

Careful design of mechanical and thermal transport properties of elastomer pads in a spinning disk scan system can provide improved heat transfer during high-power implantation. Use of a dedicated IR sensor provided in-situ measurements of wafer/pad temperatures during and directly after high-dose implants. Control of wafer temperatures below 35 C during implant was found to be beneficial for improving bipolar transistor gain in high-performance IC devices.

REFERENCES

[1] D.K. Sadana, M.I. Current, "Fabrication of Silicon-on-Insulator (SOI) and Strained-Silicon-on-Insulatortor (sSOI) wafers using ion implantation", in Ion Implantaiton: Science and Technology, ed. J.F. Ziegler, Ion Implamtatation Technology, Co. (2006). 8-1 to 8-28.

[2] E.J.H. Collart et al., "Process characterization of low temperature ion implantation using ribbon and spot beam on AIBT iPulsar high current", IIT10, AIP Proc. 1321 (2010) 49-52.

[3] M. LaFonaine, N. Tokoro, J.P. O'Connor, "Wafer temperature and stress profiles in an MeV ion implanter using the finite-element method", IIT96, IEEE Proc. 96TH8182 (1996) 583-586.

[4] K. Kandatsu, "Wafer temperature correction system for ion implantation device", US Patent US 8,552,409 B2 (Oct. 8, 2013; Assigned Texas Intruments).

[5] K. Larson, "Improved cooling on the Varian VIISta series ion implanters", IIT2000, IEEE Proc. 00EX432 (2000) 439-43.

[6] http://en.wikipedia.org/wiki/Shore_durometer.

[7] L. Pelaz, L.A. Marques, J. Barbolla, "Ion-beam-induced amorphization and recrystallization in silicon", J. Appl. Phys. 96(11) (2004) 5947-5976.

[8] K.R.C. Mok et al., "Comprehensive model of damage accumulation in silicon", J. Appl. Phys. 103 (2008) 014911.